We are IntechOpen,
the world's leading publisher of
Open Access books
Built by scientists, for scientists

6,100
Open access books available

167,000
International authors and editors

185M
Downloads

Our authors are among the

154
Countries delivered to

TOP 1%
most cited scientists

12.2%
Contributors from top 500 universities

CLARIVATE ANALYTICS
BOOK CITATION INDEX
INDEXED

WEB OF SCIENCE™

Selection of our books indexed in the Book Citation Index
in Web of Science™ Core Collection (BKCI)

Interested in publishing with us?
Contact book.department@intechopen.com

Numbers displayed above are based on latest data collected.
For more information visit www.intechopen.com

Chapter

Novel Composites for Bone Tissue Engineering

Pugalanthipandian Sankaralingam, Poornimadevi Sakthivel and Vijayakumar Chinnaswamy Thangavel

Abstract

Novel metal oxide-doped fluorophosphates nano-glass powders were synthesized by melt quenching method, and their non-toxicity is proved by MTT. Their efficacy in bone formation is confirmed by osteocalcin and ALP secretion. Composites were made using PLA, PDLLA, PPF, or 1,2-diol with fluorophosphates nano-glass powders (AgFp/MgFp/ZnFp). Their non-toxicity was assessed by cell adhesion and MTT. The ability of the composite for bioconversion was assessed by RT-PCR estimation for osteocalcin, Collagen II, RUNX2, Chondroitin sulfate, and ALP secretion accessed by ELISA method. The animal study in rabbit showed good callus formation by bioconduction and bioinduction. The bioconversion of the composite itself was proved by modified Tetrachrome staining. From the 12 different composites with different composition, the composite PPF+PDLLA+PPF+ZnFp showed the best results. These obtained results of the composites made from common biological molecules are better than the standards and so they do biomimic as bone substitutes. The composites can be made as strips or granules or cylinders and will be a boon to the operating surgeon. The composite meets nearly all the requirements for bone tissue engineering and nullifies the defect in the existing ceramic composites.

Keywords: fluorophosphate, nano bioactive glass, bioconversion, bone substitute, synthetic bone graft

1. Introduction

Scientists have tried natural polymer, synthetic polymer, various ceramics, and composites, etc., as bone graft substitutes. An ideal bone substitute should be non-toxic, osteoconductive, osteoinductive, bioconvertable, physical properties should be near to that of normal bone, should be cost-effective, easily sterilizable, and be feasible for bulk production. The commonly available bone graft substitutes do not meet all the above requirements [1, 2].

The materials that were put to use initially were ceramics (hydroxyapatite and tricalcium phosphate) as bone graft substitutes. Hydroxyapatite was only

osteoconductive and rarely was converted to bone even after years [3, 4]. It was not useful in replacing weight-bearing function. Tricalcium phosphate had minimal osteoinductive capacity along with osteoconduction but had no bioconversion capability [5, 6].

To have the advantage of bioconversion, certain specific bone hormones such as "Bone Morphogenic Protein" (BMP) came into use. "Demineralized Bone Matrix" (DBM) was also marketed as bone graft substitute, which was discovered by Urist [7]. The essential problem in their use is the phenomenal cost involved, and they had good osteoinduction but were not good osteoconductors. Hench [8] came out with the 45S5 glass, which was a breakthrough as it was made from cheap chemicals, was osteoconductive as well as osteoinductive, was able to merge with the natural bone, and is commercially available. The drawback with 45S5 glass is their very slow resorption, the longer time taken for bioconversion, and their inability to be used as a weight-bearing implant. The time taken for bioconversion was a drawback in reducing the duration of morbidity of the patients. To circumvent these problems, silica-free phosphate bioglasses and metal-oxide-doped bioglasses entered into these fields.

Over decades, orthopedic surgeons know chronic ingestion of fluoride in abundance leads to fluorosis, an ectopic bone-forming condition [9]. This was used to our advantage, and the ideal concentration of fluoride in the ceramics network was standardized. The evaporation of fluorine from the fluoride compound was circumvented by the new methodology of preparing fluoride bioglasses by melt quenching.

Standardization of the ideal mole percentage of fluoride resulted in the invention of fluorophosphates glasses, which are much more bio active than other types of phosphate and silica glasses and had a higher rate of bioconversion and faster resorption [10, 11]. Doping them with metal oxides improved their physical properties and brought the elastic moduli close to that of the human bone. Scaffolding the fluorophosphate glasses was essential to bring the molecule for clinical use that will bridge the gap between the need of the surgeon and the capability of the scientist.

This novel synthetic composite is made from bioinert polymers comprising poly lactic acid, poly D, L -Lactic acid, and bioactive polymers consisting of polypropylene fumarate, diester of fumaric acid, and 1,2 propylene diol and a bioactive inorganic component consisting of a metal-doped fluorophosphates nano glass powder. It can be fabricated as granules, scaffolds such as strip and cylinder. The plurality of the shapes that can be made gives additional advantage to the surgeon.

The standard biomaterial should mimic the biological process in the microenvironment simply denoted as "Biomimetics." The selected three different metals have beneficial properties as follows: (a) Silver: The best antimicrobial agent is especially in wound healing and skin care. (b) Magnesium: It plays a vital role in bone structure development and also acts as dietary supplement in medicine. (c) Zinc: It involves in DNA synthesis, gene expression, and wound healing. Also, the degradation products of the biocompatible polymers (PLA, PDLLA, PPF, and 1,2-diol) all enter the Kreb's cycle and excreted. So, the metal oxides and the polymers induce bone formation by stimulating the genetic pathway of bone formation and so are biomimetic.

2. Materials

Poly lactic acid (PLA) and poly DL-lactic acid (PDLLA) were procured from BioDegmer® Japan. Polypropylene fumarate (PPF) was prepared by transesterification method [12]. The di-1,2-propanediol ester of fumaric acid (1,2-diol) was prepared by azeotropic distillation, and its detailed explanation is available in previous publication [13].

The fluorophosphate glasses were prepared by melt quenching method and converted to nano particles by mechanical milling. The measured quantities of the required chemicals (Na_2CO_3, $CaCO_3$, CaF_2, P_2O_5, and $ZnO/Ag_2O/MgO$) were taken in a ball mill and homogenized. The mixture was heated in a 10% alumina crucible for 1 h up to 120°C and cooled to room temperature. The material was again ball milled for 1 hr. The components were taken in a platinum crucible and kept in a furnace preheated to 1100°C for 90 min. Then the crucible with the material was quenched by plunging in liquid nitrogen. The formed glass was broken to pieces and milled for 48 h to obtain metal-oxide-doped nano powder of the specific fluorophosphates glass [14].

2.1 Gel foam casting under rapid heating

The required amounts of the PLA [15], PDLLA, PPF/1,2-diol, and AgFP/ZnFP/MgFP were taken and dispersed in dichloromethane using a magnetic stirrer (300 rpm). Once the mixture was homogenized, the material was slowly poured over a hot glass plate (70°C). The rapid evaporation of dichloromethane leads to the generation of random pores in the composite scaffold formed. After complete evaporation of the solvent, highly interconnected porous scaffold with homogeneous distribution of the components was obtained. The scaffold thus made can be ground to granules, cut into strip, or rolled into cylinder [16].

To know the significance of PDLLA, scaffolds were fabricated with or without PDLLA [17]. The fabricated composites are: 1. PLA+1,2-diol+AgFp, 2. PLA+PDLLA+1,2-diol+AgFp, 3. PLA+PPF+AgFp, 4. PLA+PDLLA+PPF+AgFp, 5. PLA+1,2-diol+ZnFp, 6. PLA+PDLLA+1,2-diol+ZnFp, 7. PLA+PPF+ZnFp, 8. PLA+PDLLA+PPF+ZnFp, 9. PLA+1,2-diol+MgFp, 10. PLA+PDLLA+1,2-diol+MgFp, 11. PLA+PPF+MgFp, 12. PLA+PDLLA+PPF+MgFp.

3. Methodology

3.1 In vitro evaluation of the scaffolds

3.1.1 Metal-doped fluorophosphates nano bioglasses.

The biological activity (cell viability, attachment, and proliferation) of the metal-doped fluorophophate nano bioglass was ascertained by cell adhesion and MTT assay; Potential osteogenic differentiation was ascertained by (Alkaline Phosphatase Activity) and non-collagenous protein (intra and extracellular osteocalcin) of the nano glass, in relation with MG63 cell lines.

3.1.2 Scaffolds (PLA+PDLLA+PPF/1,2-diol+AgFp/ZnFp/MgFp)

The significance of the pores in the scaffold was assessed by calcein AM study and MTT evaluation. By following standard Kokubo protocol, simulated body fluid

(SBF) was prepared. All the fabricated scaffolds were cut into $2X2cm^2$ size. The scaffolds were placed in 20 mL SBF filled glass container, for a period of 21 days at 5% CO_2 incubator (Heraus – Germany). The pH variation was noted everyday using pH meter E1 model. After 21 days, the scaffolds were carefully removed; dried in laminar air flow for 48 h. The variation in the pH over 21 days was noted. The deposition of hydroxyapatite and fluorapatite was investigated by FTIR and SEM_EDAX. The toxicity of the different composites with different composition of the components was ascertained by the MTT in relation to the SaOS2 and human endothelial cell lines. Their efficiency in enhancing secretion of alkaline phosphatase and chondroitin sulfate, the ground substance of the bone was measured by ELISA method. The ability of the composites in the secretion of osteocalcin, Collagen II, RUNX2 was assessed by RT-PCR method. The porosity and micro-architecture in the multilayered scaffold were assessed by Micro-CT evaluation with GE SRμCT analyzer.

The primers used for PCR were as follows:

- Collagen type II

- Forward primer: CATGAGGGCGCGGTAGAGA.

- Reverse Primer: ATCCCCTCTGGGTCCTTGTT.

- Product length: 296.

- Osteocalcin.

- Forward primer: TCACACTCCTCGCCCTATTG.

- Reverse Primer: CTCTTCACTACCTCGCTGCC.

- Product length: 132.

- RUNX2Sequence (5′- > 3′) Template strand Length Start Stop Tm GC% Self complementarity Self 3′ complementarity.

- Forward primer CCACCGAGACCAACAGAGTC Plus.

- Reverse primer GTCACTGTGCTGAAGAGGCT.

- Product length: 119.

The analysis of the results was performed using ABI PRISM® 7000 Sequence Detection System software that enables more sensitive and accurate estimation of the relative gene expression.

3.2 In vivo studies

3.2.1 For granules

The *in vivo* studies were conducted with the Ethics committee approval (Ethical committee approval no. ABS/IAEC/18-10-2019/003-). A single species

of *Orictologuscuniculus* was purchased from King Institute, Chennai, India, and domesticated over a period of 2 weeks. The day-night rhythm was maintained and was fed on good nourishing food. The adaptation was confirmed by the gain in weight of 150 g in 2-week time. (1800–1950 g).The composite (PLA+PDLLA+PPF+AgFp) granules were prepared by grounding the scaffold and sterilized by ethylene oxide gas.

The animal was given a premedication of pedichloryl syrup (2.5 mL) 30 minutes before surgery. Intramuscular ketamine anesthesia was given in the dose of 45 mg per kilogram body weight and waited for 10 minutes to get the full dissociated anesthetic effect. The anesthetic effect was maintained by oxygen and sevoprim inhalation through mask (**Figure 1**).

The left thigh was repeatedly painted with 10% povidone iodine and ethylene alcohol. Xylocaine 2% with adrenaline was injected in the line of incision as an additional analgesia and also a hemostatic agent. The skin incision made on the anterolateral aspect was rolled down to expose the posterior boarder of the quadriceps muscle. Using sharp dissection, the muscle was slit open and enlarged by thin bone spikes to expose the anterolateral aspect of the thigh bone. Using an electric dental burr of 1 mm, a trough was made for a length of 2 cm.This exposed the medullary cavity. It was packed with the sterile composite powder. Liberal saline wash was given to wash off the spilled over composite materials. The spikes once removed the muscle fell back into position completely covering the bony trough. The two 3–0 vicryl stitches were used to close the muscle. The skin incision, which was far away from the bone work, was closed with 3–0 ethilon. A single dose of ceftrioxazone 250 mg was given intramuscularly.

3.2.2 For strip

The *in vivo* studies were conducted with the Ethics committee approval (Ethical committee approval no. ABS/IAEC/18-10-2019/003-). Three male rabbits were
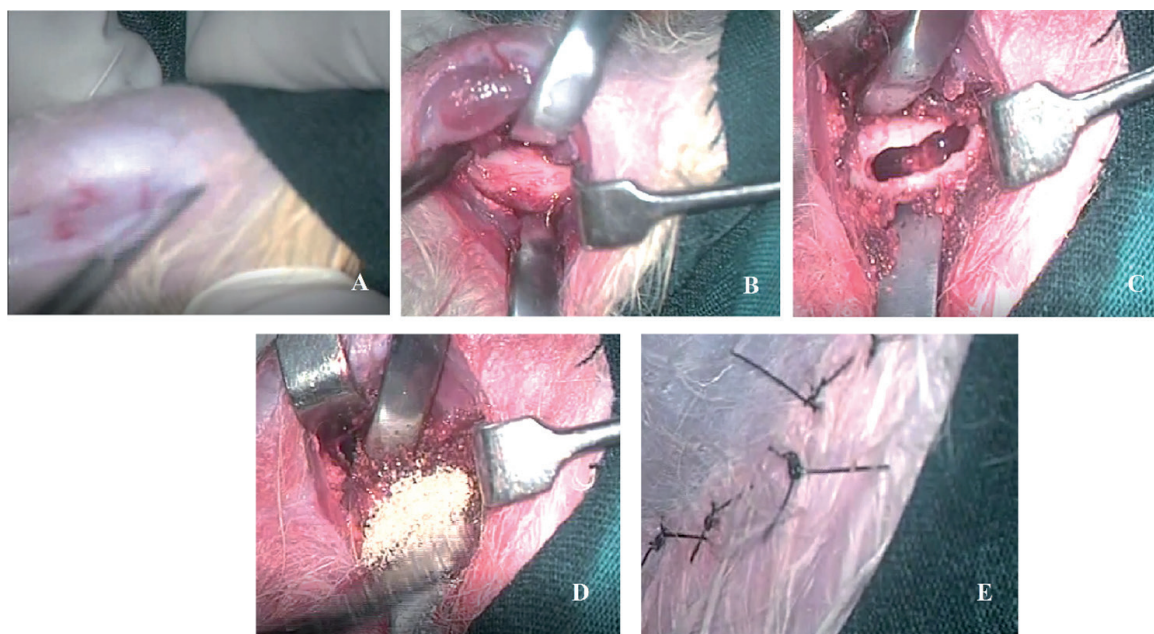

Figure 1.
In vivo study in rabbit (granules-PLA+PDLLA+PPF+AgFp) [A-thigh preparation, B - femur exposed, C - gutter in the femur, D - gutter filled with granules E - Wound closed by sutures.
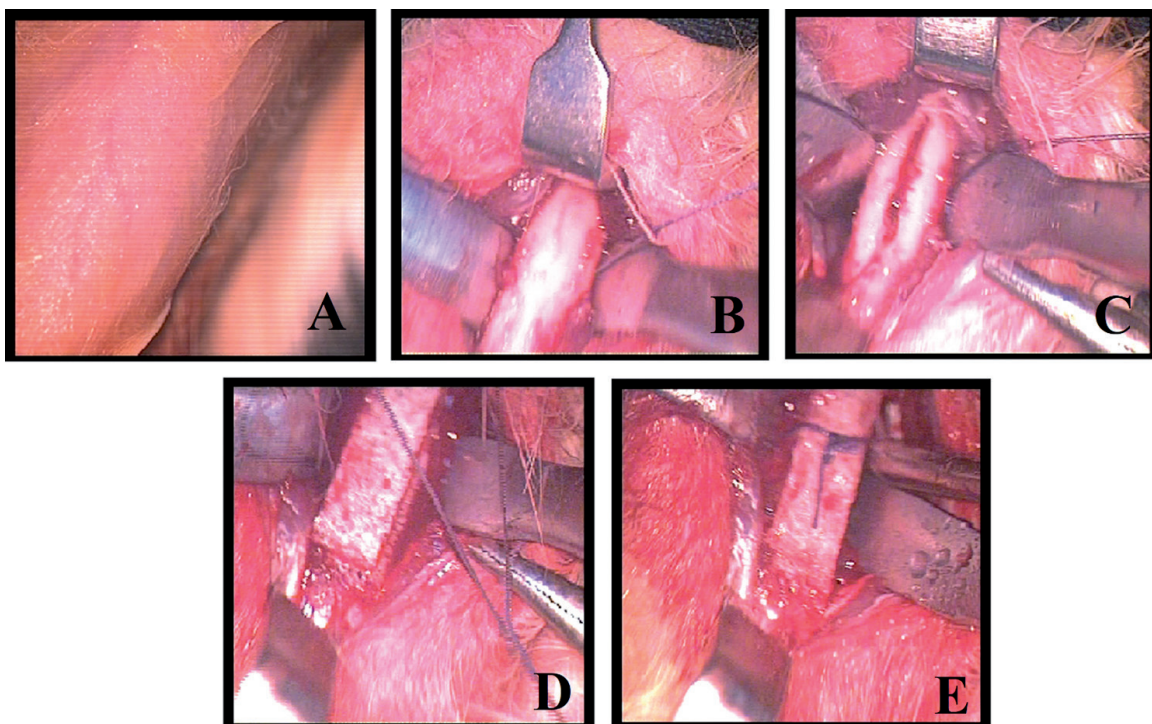
Figure 2.
In-vivo study in rabbits (strip -PLA+PDLLA+PPF+AgFp). [A - Thigh preparation, B - Femur exposed, C - Cut in the femur, D - Two strips one above another over the cut, E - Maintain position by vicryl knot].

procured and domesticated in the same way as explained before. The AgFp/ZnFp/MgFp composites were made with PLA+PDLLA+PPF by gel foam casting under rapid heating. They were of 1 mm thickness and cut into size of 2X20mm. The cut specimens were sterilized by ethylene oxide gas sterilization.

The animals were anesthetized, limb prepared, and femur exposed as described in the previous section. Narrow cuts were made with no.701 conical dental burr at an angle of 45° to the femur to make it extremely thin cut. The 3–0 vicryl was threaded around the femur and both the ends were kept free. Two layers of the 2X20mm sterilized composite strips were kept over the cut made allowing the marrow blood to soak the specimen. The vicryl was tied around the specimen so that the specimen does not slip or move away and the wound was closed in layers. The procedure was done for all the three specimens, one on each animal (**Figure 2**).

The animals were cared for the postoperative period with nourishing food. The day 1 X-ray did not show the specimen in either view as the specimens were translucent to the X-ray. The X-ray evaluation was done under sedation on the first, ninth, and 16th day. Clinical union occurred as early as the 15th day. The CT evaluation was done on the 19th day. The animals were euthanized as per the protocol and the limb harvested, denuded of skin and muscles, and bone preserved in 10% formalin. The X-rays of the specimens taken and then sent for histopathological evaluation in both EH stain and modified tetrachrome stain. The procedure adapted is shown in the serial photographs in **Figure 2**, where two layers of 1 mm thick strips have been placed over a very narrow corticotomy wound in the shaft of femur and have been retained in position by a single 3–0 vicryl encircling knot.

4. Results and discussions

4.1 Metal-doped fluorophosphates nanobioglasses

Alkaline phosphatase (ALP) is an osteogenic differentiation marker at all the stages from the differentiation of the mesenchymal cells to the mineralization front. Hence its enhanced secretion is considered as a vital factor to choose the ingredient for the composite for Bone Tissue Engineering (BTE). The obtained results (**Table 1**) indicated that AgFp and MgFp showed consistently raised levels at all concentration from 0.1 to 100 μg/mL, whereas ZnFp showed increased secretion only at lower concentrations of 0.01 and 1 μg/mL [18, 19].

Bone is a composite of the ground substance reinforced by multiple collagens and mineralized by hydroxyapatite [20]. Though various collagens are present in various parts of the body, osteocalcin is found exclusively in bone. It is also an excellent gene marker of bone induction. The ability of the ionic dissolution products of various FP glasses in various concentrations was evaluated for their efficiency to promote osteocalcin secretion. While the extracellular expression of osteocalcin [21] showed increase than the control only with ZnFp and MgFp, (**Table 2**) intracellular osteocalcin was raised in most of the glasses, but significant raise was present in ZnFp, MgFp, and AgFp glasses and was more when the concentration of the products of dissolution was 10 μg/mL.

The calcein AM study was used to assess the cell wall integrity and the double staining to assess the cytotoxicity showed specific features. The control group of cells was not only brilliantly green but also showed homogeneous spindle shape, indicating the integrity of cell wall and the metabolic potential. The addition of PPF to the basic

Samples	ALP (μg/mL)			
	0.1	1	10	100
AgFp	156.2	132.3	148.3	140.5
ZnFp	136.8	139.6	125.5	129.8
MgFp	143.7	143.4	148.0	138.3
Control			130.3	

Table 1.
Alkaline phosphatase activity of metal-doped fluorophosphates nano bioglass powders.

Samples	Intracellular (Concentration (μg/mL))			Extracellular (Concentration (μg/mL))		
	1	10	100	1	10	100
AgFp	0.091	0.084	0.207	0.319	0.194	0.274
ZnFp	0.011	0.251	0.000	0.208	0.557	0.324
MgFp	0.091	0.084	0.207	0.469	0.300	0.317
Control	0.083	0.083	0.083	0.430	0.430	0.430

Table 2.
Osteocalcin (intracellular and extracellular) activity of metal-doped fluorophosphates nano bioglass powders.
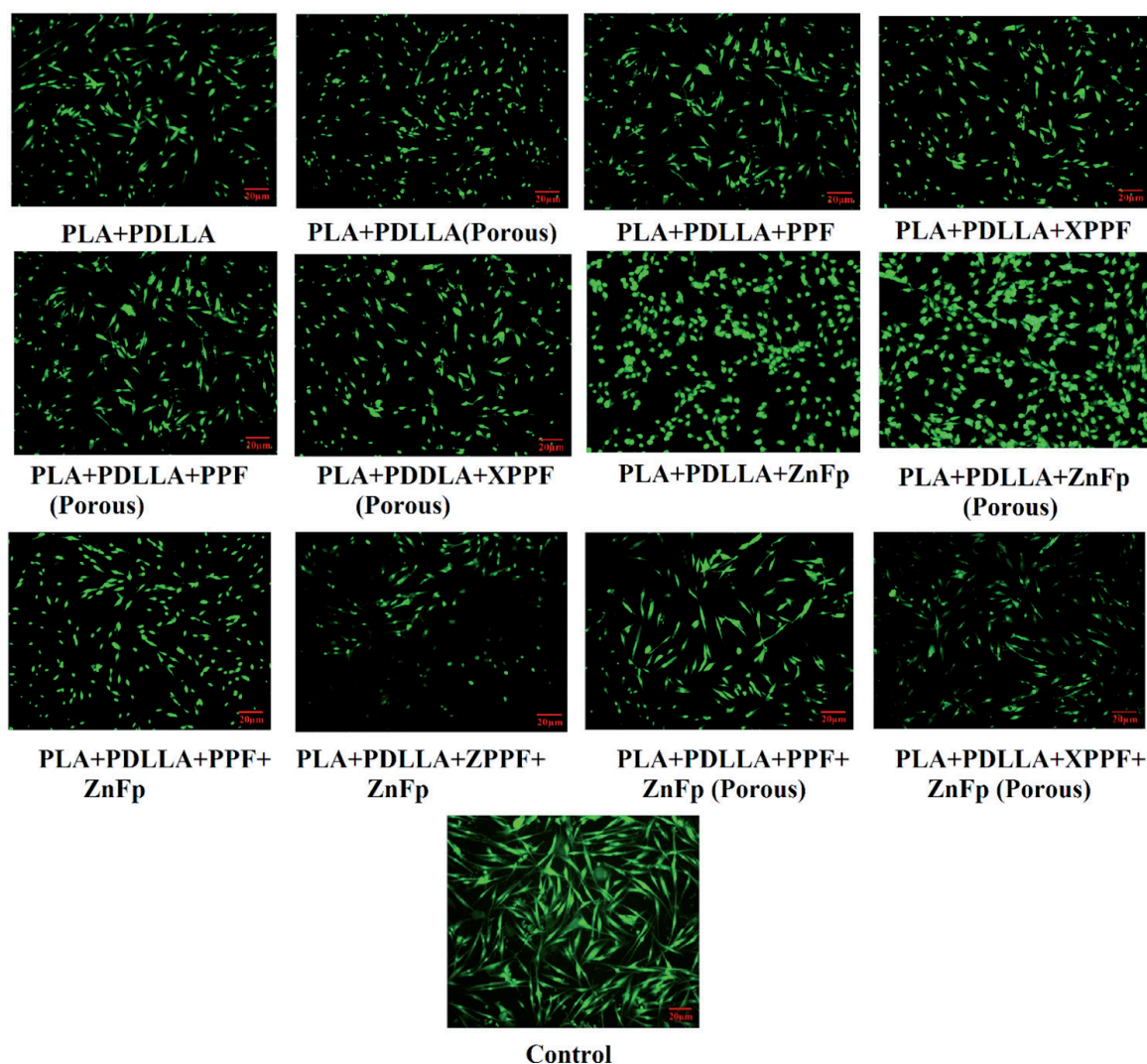
Figure 3.
Calcein AM study of composites.

components PLA+PDLLA increased the cell wall integrity and the addition of pores to the same increased the number of spindle shaped cells [22].

The addition of FP glass to the basic components PLA+PDLLA [23] with pores or without pores increased the number of cells phenomenally, but the quality of them was poor exhibited by their round shape rather than the spindle shape of the healthy cell. When all the components PLA+PDLLA+PPF and ZnFp glasses were added, both the intensity of fluorescence and the quality of the cells also increased, and it was more so when pores were present in the composite (**Figure 3**).The XPPF (cross-linked PPF) when replaced the PPF in the composite, there was only deleterious effect both in the fluorescence and the quality of the cells (**Table 3**).

From the above study, it can be inferred that the least toxic composite was that of PLA+PDLLA+PPF+ZnFp glass.

The three essential gene markers in the synthesis of bone from the stage of mesenchymal stem cells to that of the osteocyte maturation are Osteocalcin [24], Collagen II [25], and RUNX2 [26](**Table 4**). When the results were charted to scrutinize the fold change than the control, the fold increase in collagen II was highest with PLA+PDLLA+PPF+AgFp, and the highest fold increase in osteocalcin was also with AgFp but when constituted with 1,2-diol than with PPF. The highest fold change in

Sample name	Mean	SD	% Cytotoxicity
PLA+PDLLA	50.60	0.19	49.40
PLA+PDLLA(porous)	48.21	1.21	51.79
PLA+PDLLA+PPF	43.70	0.78	56.30
PLA+PDLLA+XPPF	59.18	1.79	40.82
PLA+PDLLA+PPF+ZnFp	87.11	1.20	42.89
PLA+PDLLA+XPPF+ZnFp	42.70	1.36	57.30
PLA+PDLLA+PPF(Porous)	51.79	1.21	48.21
PLA+PDLLA+XPPF(Porous)	60.69	1.51	39.31
PLA+PDLLA+PPF+ZnFp(Porous)	78.37	3.92	21.63
PLA+PDLLA+XPPF+ZnFp(Porous)	69.53	1.71	30.47
PLA+PDLLA+ZnFp	54.23	0.47	45.77
PLA+PDLLA+ZnFp(Porous)	37.99	1.64	62.01

Table 3.
Cytotoxicity of the prepared composites.

Composites	MTT	ALP (IU/mL)	CollagenII (Fold increase)	Osteocalcin (Fold increase)	RUNX2 (Fold increase)	Chondroitin levels (ng/mL)
PLA+1,2-diol+AgFp	90.95	0.443	0.16	2.30	0.04	7.450
PLA+PDLLA+1,2-diol+AgFp	79.84	1.915	0.81	4.70	0.55	11.540
PLA+PPF+AgFp	81.48	0.596	0.40	0.22	0.03	3.250
PLA+PDLLA+PPF+AgFp	81.13	1.406	4.40	3.20	0.50	5.430
PLA+1,2-diol+ZnFp	89.72	0.938	0.12	0.07	0.01	10.210
PLA+PDLLA+1,2-diol+ZnFp	84.36	2.306	1.70	1.20	0.40	3.850
PLA+PPF+ZnFp	93.42	0.503	0.50	1.40	0.09	13.230
PLA+PDLLA+PPF+ZnFp	87.20	1.543	1.10	2.60	0.98	9.780
PLA+1,2-diol+MgFp	90.54	1.081	0.25	0.05	0.78	10.880
PLA+PDLLA+1,2-diol MgFp	81.48	1.208	0.93	0.19	0.78	8.210
PLA+PPF+MgFp	53.09	1.39	0.23	0.23	0.21	5.430
PLA+PDLLA+PPF+MgFp	86.42	1.544	0.53	0.24	0.20	10.210
Control	100	1.529	—	—	—	0.180

Table 4.
MT, ALP, collagen II, osteocalcin, RUNX2, and chondroitin sulfate levels of composites.

RUNX2 than the control was with ZnFp when combined with PLA+PDLLA+PPF. All the Mg-based composites fared poorly with all the three types of gene markers (**Figure 4** and **Table 4**).
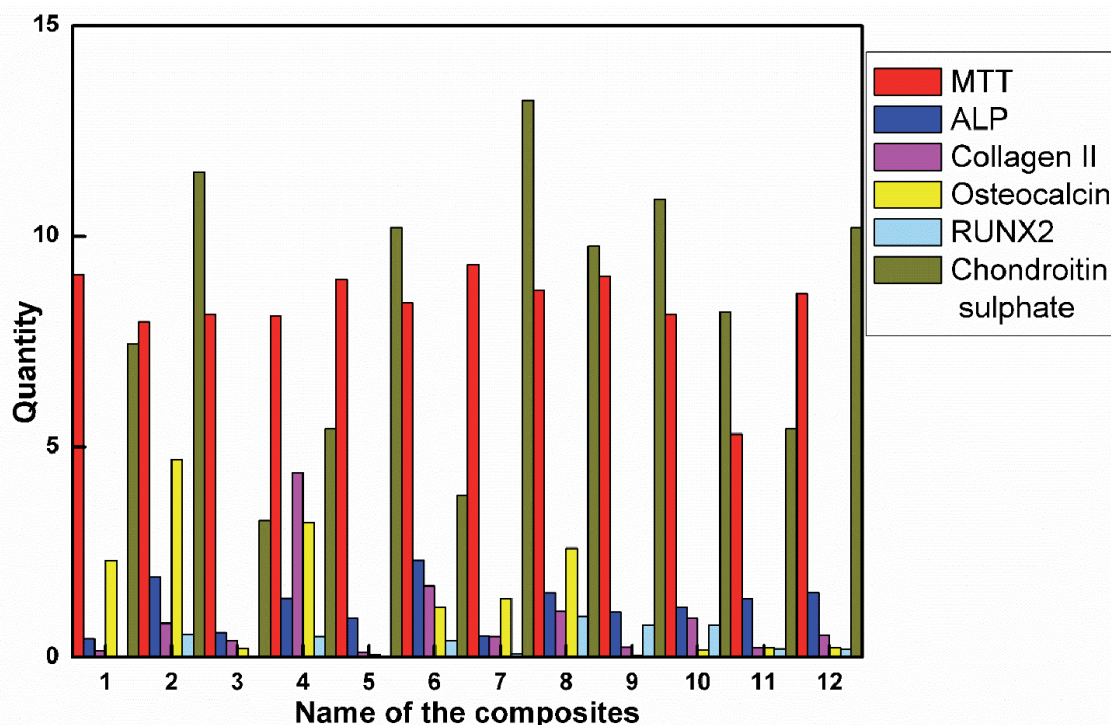
Figure 4.
Pie chart of the MTT, ALP, collagen II, osteocalcin, RUNX2, and chondroitin sulfate levels of composites of varying composition.

The results showed that all the 12 composites showed many fold increase in the secretion of chondroitin sulfate [27] than the control, immaterial of the component having 1,2-diol or PPF and the FPglass being either Ag, Zn, or Mg.

The pH variation of all the compression-molded specimens showed uniformly a reduction in the first 2 days, which is because of phosphoric acid formation. And all the specimens bounced back to 7 on the third day due to the alkaline earth metal (Na^+ and/or Ca^{2+}) release. The dissolution of the ions thus replaces H^+ ions by cations (Na^+ and/or Ca^{2+}) leading to an increase in hydroxyl ion concentration. None of them went below 6.5 even in the first 2 days. From then on it showed a steady variation between 7 and 6.7.

The strip and cylinders made by gel foam casting under rapid heating showed a better pH even in the first 2 days and never went below 6.8, and the end stage also showed higher pH than the scaffolds. The highest pH reached was with the strip of scaffold made by rapid heating method, and it was 7.15. This variation shows the better homogenezity and the porosity achieved by the rapid heating method, which avoids high acidic environment that can lead onto graft rejection[28]. The crystal formation over the strip and cylinder after *in vitro* evaluation is shown in **Figure 5**.

The predominant functional groups present in the composites were studied using their respective FTIR spectra:alcohol (3200–3500 cm^{-1}), alkanes (2850–3000 cm^{-1}), saturated ketone (1735–1750 cm^{-1}), alkenes (1630–1680 cm^{-1}), asymmetric methyl bend (1450–1470 cm^{-1}), and methyl bending (1350–1395 cm^{-1}). The presence of P-O bend (560–500 cm^{-1}) bands indicates the formation of calcium phosphate(CaO-P_2O_5) layer. The carbonate group $(CO_3)^{2-}$ (1400–1550 cm^{-1}) bands showed the crystalline
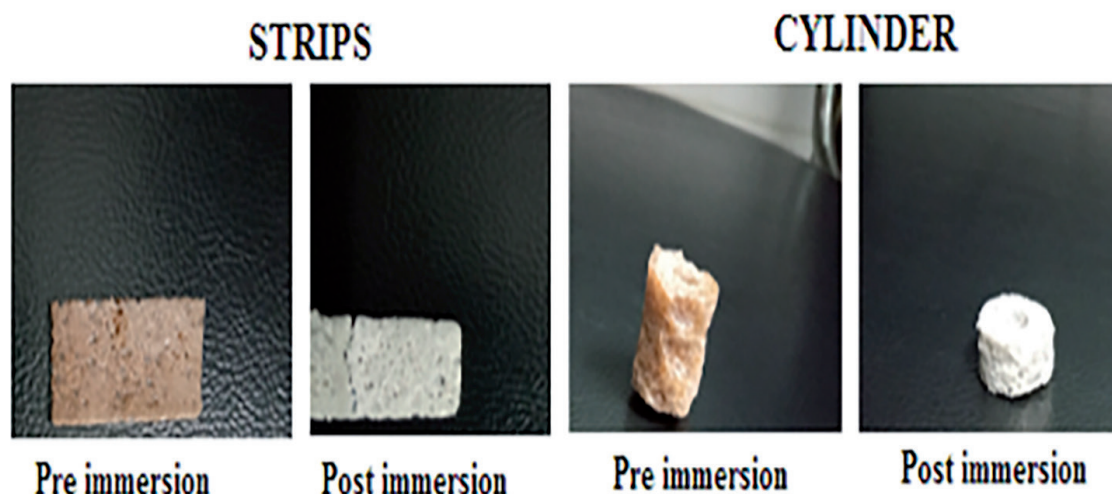
Figure 5.
Pre- and post-immersion photographs of the strip and cylinder.

nature of the HAp layer. The bands are observed at above 3500 cm^{-1}, which corresponds to the OH group. After 21 days of soaking in SBF, the strong intensity and frequency shift of the $(CO_3)^{2-}$,P-O-P stretch and P-O bend groups reveal the interaction of the composite and HAp precipitation [29].

The shoulder peak at 1450–1410 cm^{-1} coupled with the weaker peak at 870–875 cm^{-1} corresponds to type B carbonate vibrations, whereas the vibration regions of type A carbonate are 1450–1410 cm^{-1} coupled with a band at 880 cm^{-1}. The type A and B carbonates [30, 31] are indistinguishable in these scaffolds because the ester peaks also lie on the same region. Both type A and B carbonates are present in these scaffolds and their intensities are maximum at three selected scaffold composites (PLA+PDLLA+PPF+ZnFp, PLA+PDLLA+PPF+AgFp, PLA+PDLLA+PPF+MgFp), For the same composites, the corresponding peaks for HAp in rapid heating combined gel foam casting are higher than the compression-molded scaffolds.

Although the HAp precipitation was noted in all the fabricated scaffolds, the intensity of the carbonated group $(CO_3)^{2-}$ and phosphatebased group (P-O-P asymmetric and symmetric stretch, P-O bend) was observed as high in gel foam casting under rapid heating.

The SEM evaluation of the scaffolds and strips was done after gold sputtering. (Model Ultra 55; Zeiss, Oberkochen, Germany). After evaluating the surface apatite formation, the specimens were cut into two halves and turned by 90°, and the depth of the apatite formation was measured. There was no significant change in the percentage, and it was infered that all the composites have near equal conversion once the pores allow penetration of the SBF inside except the absence of PDLLA had negative significance in the extent of crystalline conversion (**Table 5**).

The similar specimens were subjected to *in vitro* evaluations, which were analyzed by the same way in the same Scanning Electron Microscope to assess the degree of surface pores and the change in crystallinity after *in vitro* study. The photograph of a stirp of composite and a cylindrical composite, both made by gel foam casting under rapid heating, shows the retention of the shape after SBF immersion for 21 days, but there was complete change in the color and the texture indicating the crystalline conversion. The SEM of scaffold in two different magnifications both before and after *in vitro* evaluation is shown in **Figure 6**, which shows very scarce

Composites	Crystallinity(%)
PLA+1,2-diol+AgFp	86.88
PLA+PDLLA+1,2-diol+AgFp	97.42
PLA+PPF+AgFp	49.36
PLA+PDLLA+PPF+AgFp	72.70
PLA+1,2-diol+ZnFp	59.54
PLA+PDLLA+1,2-diol+ZnFp	78.89
PLA+PPF+ZnFp	87.31
PLA+PDLLA+PPF+ZnFp	76.19
PLA+1,2-diol+MgFp	73.33
PLA+PDLLA+1,2-diol MgFp	78.68
PLA+PPF+MgFp	94.62
PLA+PDLLA+PPF+MgFp	82.09
PLA+PDDLA+PPF+AgFp(Strip)	73.62
PLA+PDDLA+PPF+ZnFp (Strip)	81.42
PLA+PDDLA+PPF+MgFp(Strip)	87.34

Table 5.
Apatite conversion(%).

amount of crystallization in the pre *in vitro* evaluation and the homogeneous pores being well exhibited. After 21 days of immersion in SBF, the crystalline conversion is observed, and all the pores have been near completely clogged with the crystals formed [32, 33].

The SEM micrographs of the scaffolds (pre- and post-immersion). In pre-immersion status shows specks of crystallization indicating the high hydrophilicity of the scaffold, and the post-immersion evaluation of the same shows complete formation to crystals, which proves the high bioresorbability of the scaffold. The SEM evaluation of multilayered scaffold made by rapid heating under low magnification shows the adequacy of pores. The pre-immersion and the post-immersion SEM micrographs clearly show the formation of sufficient crystals. The EDAX evaluation of the pre and post *in vitro* SEM confirms the high level of carbonated hydroxyapatite and fluroapatite formation in the scaffold.

The Micro-CT (**Figure 7**) evaluation of the cylindrical scaffold made by gel foam casting under rapid heating proved the following factors: a) The scaffold had no layering and was continuous. b) There was adequate porosity and the pore sizes were varying. c) The pores were all well connected by interpores. The same specimen after *in vitro* evaluations had sufficient fomation of crystals with the preservation of the deeper pores [34].

4.2 *In vivo* studies

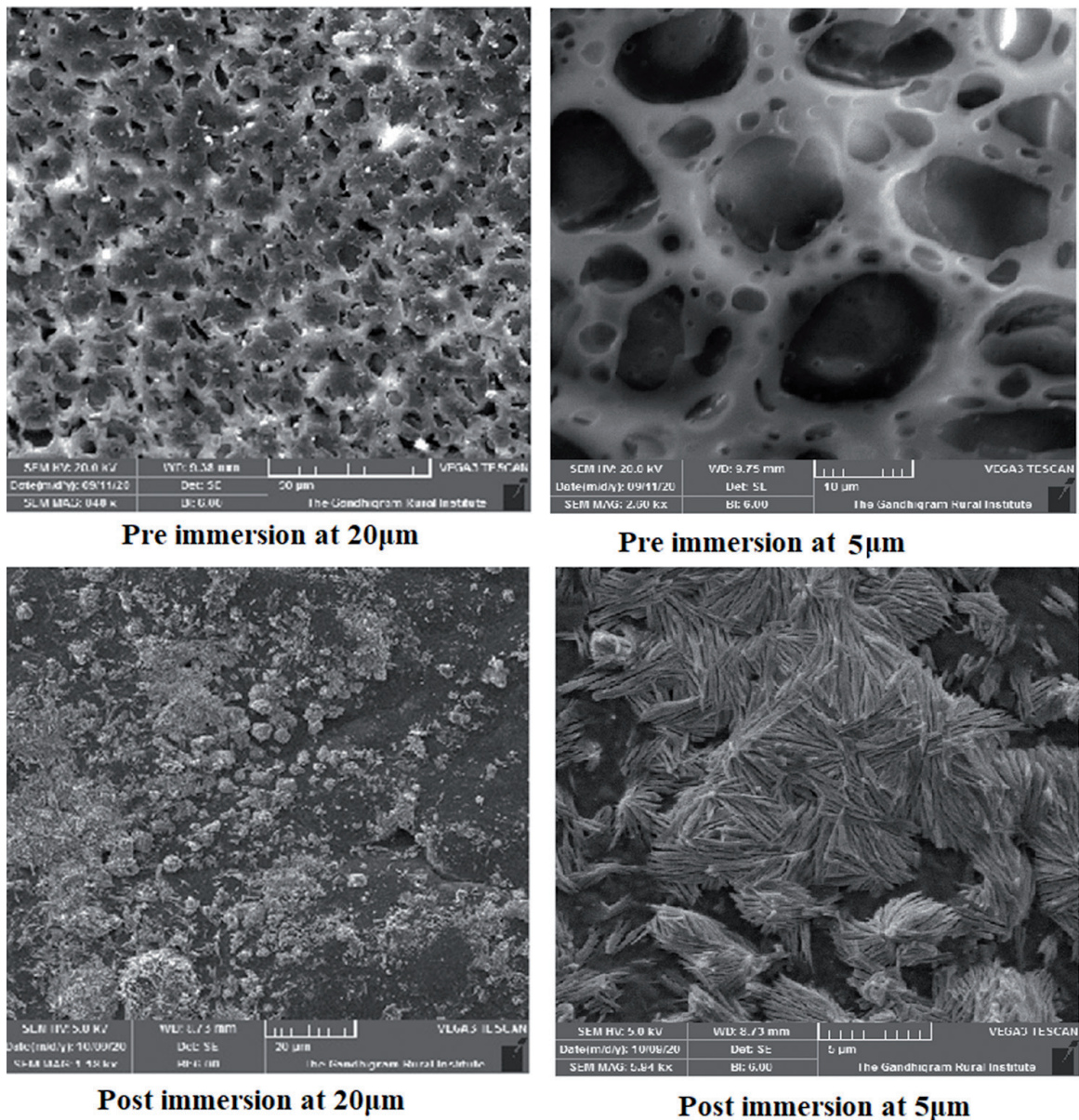From the *in vitro* evaluation, PPF-based composites were shortlisted for *in vivo* studies.

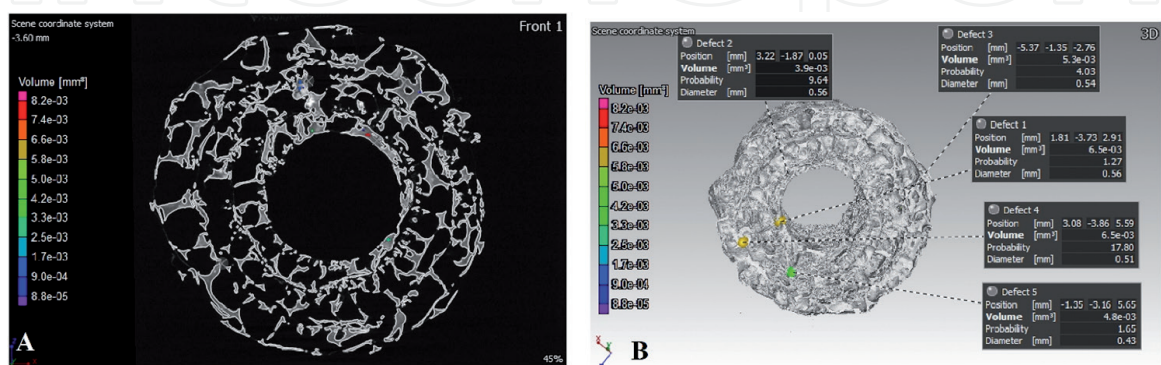**Figure 6.**
Pre- and post-immersion of the scaffolds.

Figure 7.

Micro-CT studies of the cylindrical composite. (A - Pre-immersion and B – Post-immersion).

4.2.1 Granules

It was found that the femur had fractured and the ends were apart (**Figure 8**). Neither immobilization of the femur or any form of fixation was done. The rabbit was not limping and was feeding well. There was only a flare of the ends of the fracture and there was no evidence of any callus on the ninth postoperative day. After another week (Day 16), the limb when examined clinically had sound union. The X-ray taken showed abundant callus not only in the fracture end but all along the femur where the trough had been made and even below.

The animal was euthanized, the limb harvested, skin and muscles were peeled off, and an abundant amount of callus was found to have united the fracture very strongly. The dissected specimen were studied by X-ray and the specimen were preserved in 10% formalin.

The specimen was prepared and the decalcified specimen was sectioned axially to exhibit the two segments of the femur with the intervening tissue formed. The
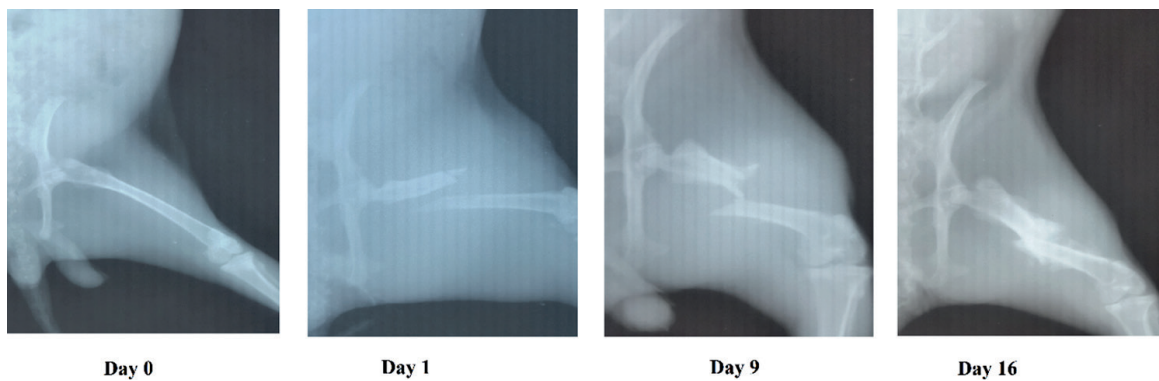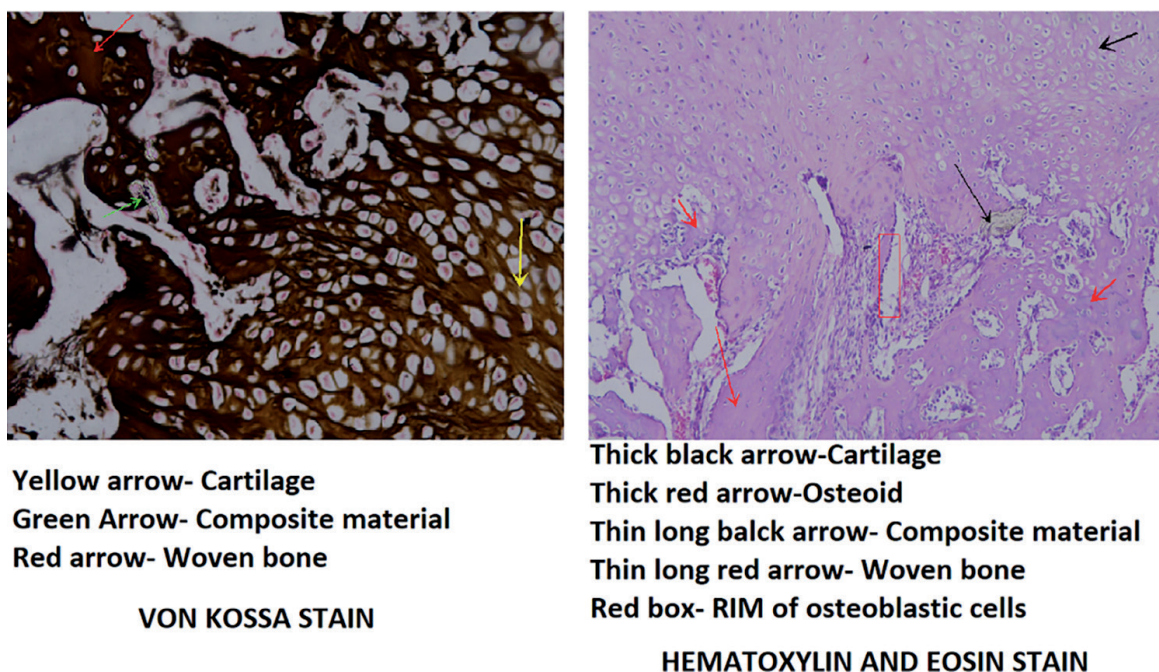

| Day 0 | Day 1 | Day 9 | Day 16 |

Figure 8.
X-ray photographs of the opearted site in rabbit.

Yellow arrow- Cartilage
Green Arrow- Composite material
Red arrow- Woven bone

VON KOSSA STAIN

Thick black arrow-Cartilage
Thick red arrow-Osteoid
Thin long balck arrow- Composite material
Thin long red arrow- Woven bone
Red box- RIM of osteoblastic cells

HEMATOXYLIN AND EOSIN STAIN

Figure 9.
Histopathological study of the dissected specimen.

specimen was stained using regular eosin-hematoxylin stain and also von kossa stain. (**Figure 9**).

The procedure done using granules of the composite has been serially shown in the photographs (**Figure 1**). Though the limb got fractured, it did not receive any specific treatment for it. Until ninth day, there was a scarce response to heal but by the 16th day it had soundly united. (**Figure 8**). The X-ray of the specimen after dissection showed the extension of the callus almost over the entire femur. The histopathological evaluation was specifically focused toward the tissue between the fractured ends where the granules had been packed. The significant observations were: a) Nearly the whole of the granules had resorbed except occasional trace of it. b) Abundant cartilage had formed between the ends indicating the enchondral ossification. c) Woven bone formed in between the ends of the fracture was a proof of the rapidity of the fusion occurring. d) The absence of multinucleated giant cells indicates the biocompatibility of the composite. e) Similar features were observed in both the staining (**Figure 9**). The modified tetrachrome staining throws much more information than the above two. a) The new lamellar bone formed in continuity with the resorbing composite granule. b) The sound union by the woven bone formed from chondral ossification. c) The abundance of osteoblasts and the osteoid. d) An exuberant neo vascularization among the fibroblasts is well seen (**Figure 10a–d**) [35, 36].

4.2.2 Strip

The X-ray photographs show no evidence of the placed composite strip or the corticotomy made as the composite is not radio opaque and the furrow is very narrow. But the X-rays taken on the ninth day showed all three animals had fractured their femur. No specific treatment such as immobilization or interference was done for the fracture. Clinical union occurred as early as 15th day and was confirmed by X-ray on 16th day (**Figure 11**) and CT scan on 19th day (**Figure 12**). The harvested limb after euthanizing
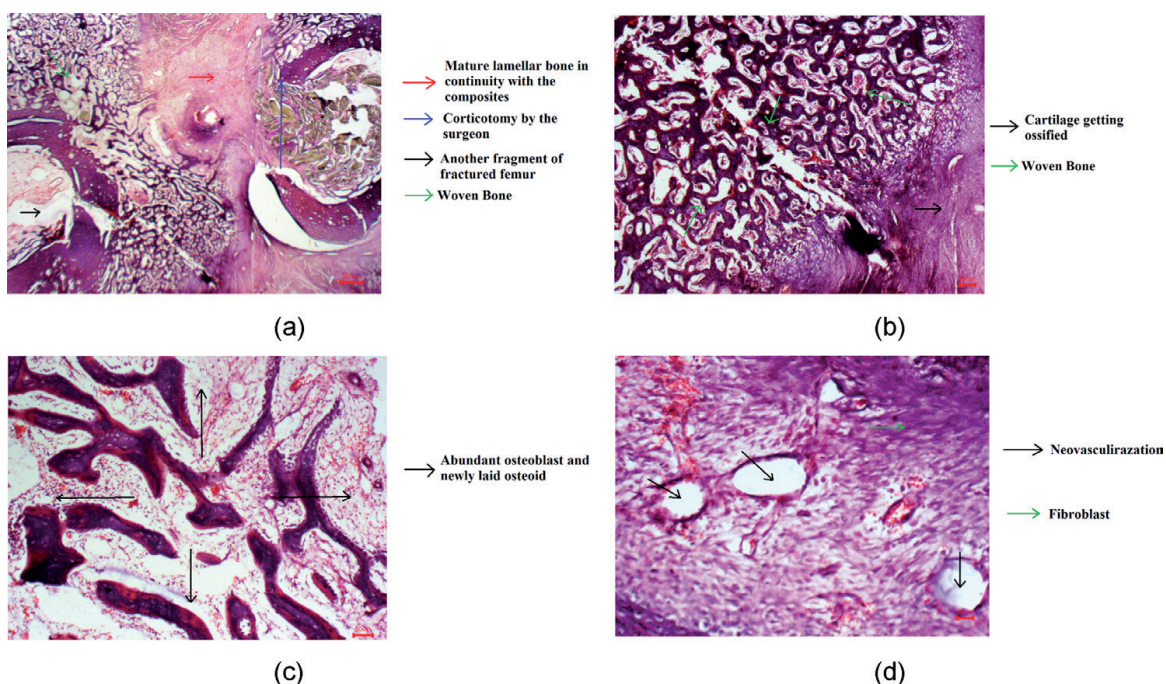

Figure 10.
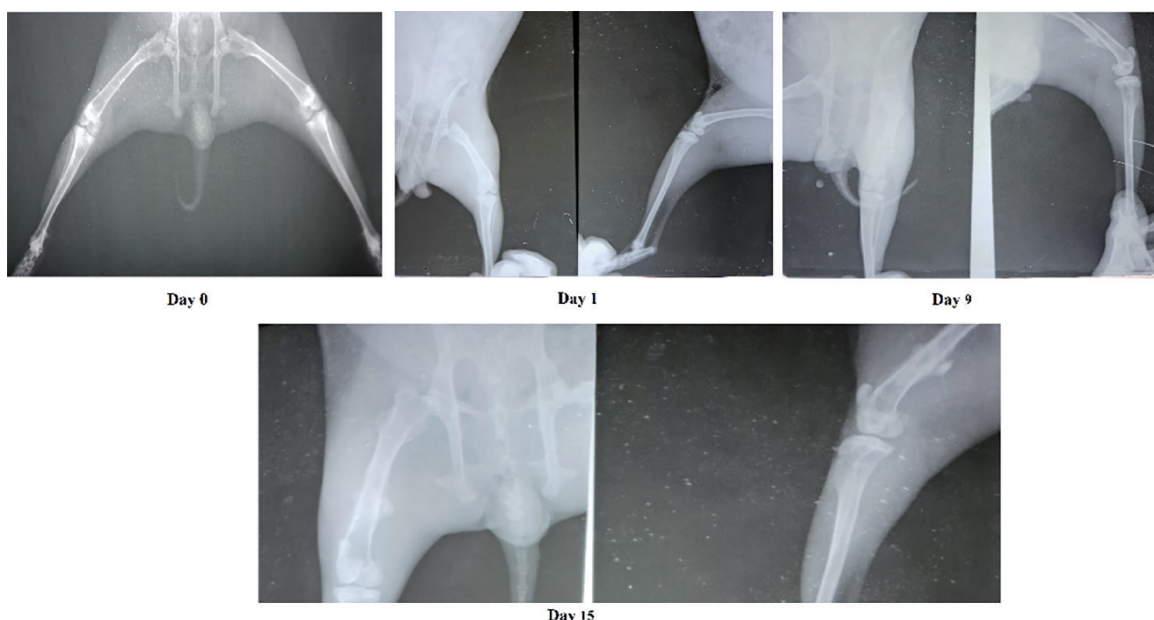*a-d represent the tetrachrome stain results of the granules (Composition: PLA+PDLLA+PPF+AgFp).*

Figure 11.
Studies using composite strips: X-ray photographs of the operated site in rabbit.
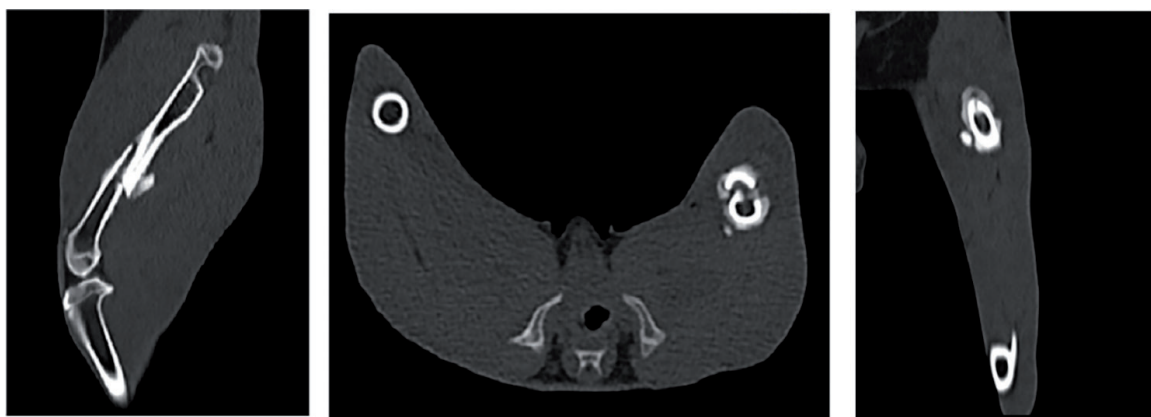

Figure 12.
Studies using composite strips: CT scan of the fractured leg in rabbit.

the animal showed the composite strip was adherent to the bone underneath. The X-ray of the specimens showed abundant callus along the fracture (**Figure 13**) and the composite strip was not seen in the X-ray.

The histopathological evaluation showed the following features: a) Both the layers of the scaffold had merged into one layer. b) The composite had attached to the bone beneath. c) There was abundant woven bone formed beneath the composite strip at the level of the corticotomy. d) The second layer of the composite strip kept away from the corticotomy had profuse infiltration of fibrocytes. e) The fibrous change-over in the superficial layer of the composite had abundant neovascularization These changes confirm the osteo induction potential of the composite, the ability of the composite to go for bioconversion, and high bioactivity of the composite [37–39].

The modified tetrachrome staining of the specimens with the cross section at the level of the composite confirmed the findings by EH stain and showed the additional features. **Figure 14a** shows conversion of the fragmented composite forming woven bone to heal the corticotomy made and the binding of the two layers of the composite
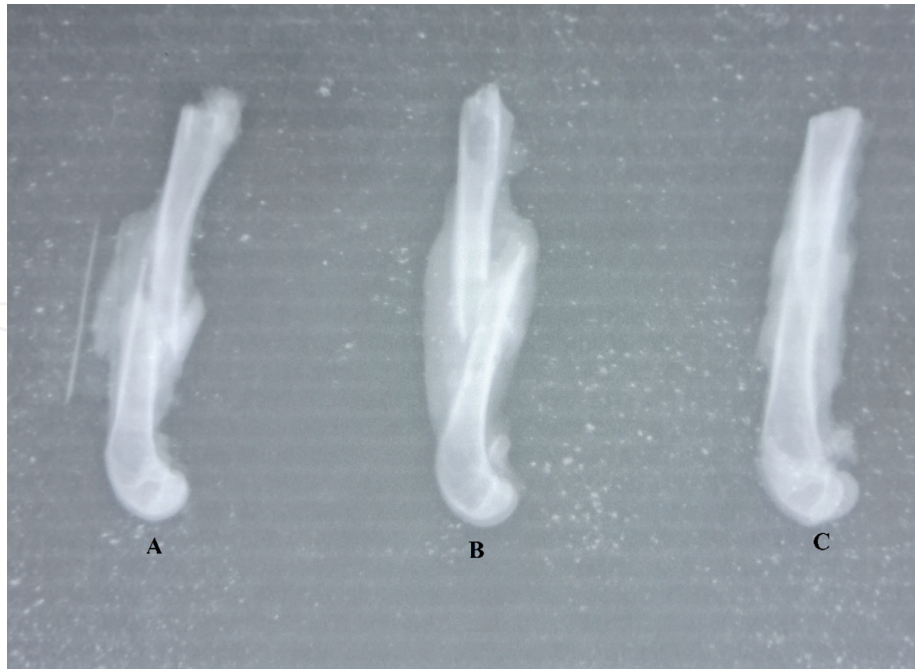
Figure 13.
Studies using composite strips: Postoperative X-ray of the dissected specimen from rabbits.
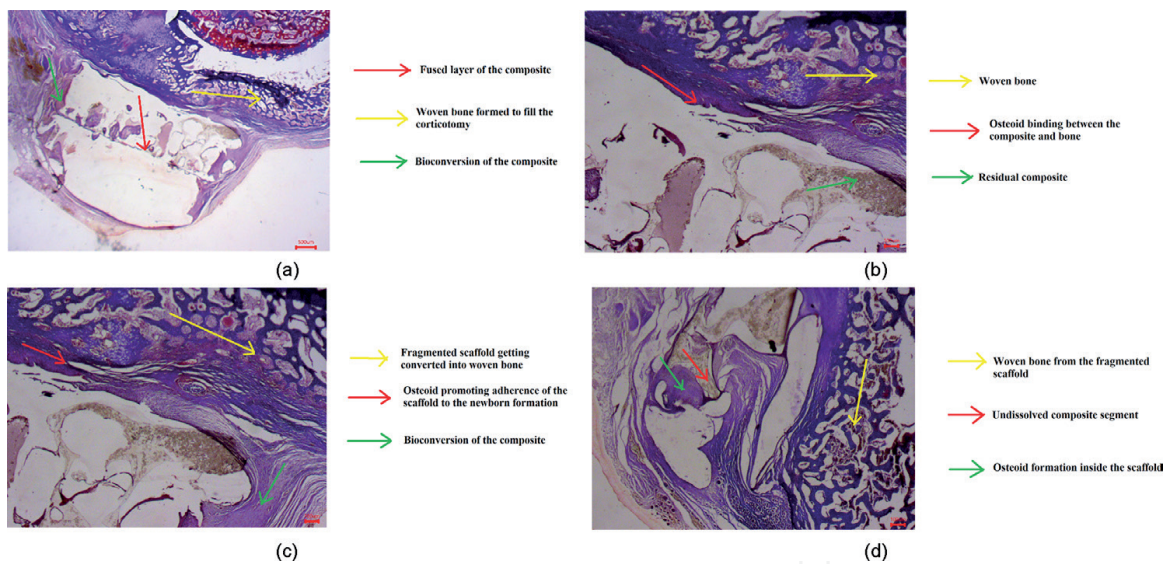*(A-PLA+PDLLA+PPF+AgFp; B-PLA+PDLLA+PPF+ZnFp; C-PLA+PDLLA+PPF+MgFp).*

Figure 14.
a-d represent the tetrachrome stain results of the strip (Composition: PLA+DPLLA+PPF+ZnFp).

strip and random infiltration of the layer close to the bone with fibroblasts and specks of osteoid. On higher magnification (**Figure 14b**), the fusion of the composite strip to the underlying bone by osteoid is well seen. On further magnification (**Figure 14c**), the infiltration of the composite by newly formed layers of osteoid is well made out replacing the dissolved area of the composite. **Figure 14d** shows the adhesion of the composite strip, the composite strip dissolving and disintegrating to form new woven bone healing the corticotomy, the abundant laying of new osteoid in the dissolved portion of the composite.

5. Conclusions

The novel composite of PLA+PDLLA+PPF+AgFp/ZnFp/MgFp meets most of the requirements of an ideal bone substitute, and it bridges the gap between the need of the clinician and the biomaterial scientist, more than the available present-day commercial ceramic composites. It is not only conductive like HAp but also inductive. It is more inductive than Tri calcium phosphate. It takes less time for resorption than Bioglass and the presence of fluoride makes the rate of bioconversion high. As the end products of all the four components of the composite are natural ingredients of the body and induce bone formation by enhancing the genetic pathway, the composite is a real biomimetics. Though small animal studies have proved the usefulness of the composite, their efficacy has to be confirmed in clinical situations in large animals before human trial.

Conflict of interest

The authors declare no conflict of interest.

Author details

Pugalanthipandian Sankaralingam*, Poornimadevi Sakthivel
and Vijayakumar Chinnaswamy Thangavel
Bone Substitutes, Madurai, India

*Address all correspondence to: drpandian@bonesubstitutes.in

IntechOpen

References

[1] Calori GM, Mazza E, Colombo M, Ripamonti C. The use of bone-graft substitutes in large bone defects: Any specific needs? Injury. 2011;**1**(42):S56-S63. DOI: 10.1016/j.injury.2011.06.011

[2] Fernandez de Grado G, Keller L, Idoux-Gillet Y, Wagner Q, Musset AM, Benkirane-Jessel N, et al. Bone substitutes: A review of their characteristics, clinical use, and perspectives for large bone defects management. Journal of Tissue Engineering. 2018;**2**(9):6819

[3] Thirumalai J. Introductory chapter: The testament of hydroxyapatite: New prospects in regenerative medicinal treatments. Hydroxyapatite. 2018;**14**: 3-14. DOI: 10.5772/intechopen.72767

[4] Apelt D, Theiss F, El-Warrak AO, Zlinszky K, Bettschart-Wolfisberger R, Bohner M, et al. *In vivo* behavior of three different injectable hydraulic calcium phosphate cements. Biomaterials. 2004;**25**(7-8):1439-1451. DOI: 10.1016/j.biomaterials.2003.08.073

[5] Theiss F, Apelt D, Brand B, Kutter A, Zlinszky K, Bohner M, et al. Biocompatibility and resorption of a brushite calcium phosphate cement. Biomaterials. 2005;**26**(21):4383-4394. DOI: 10.1016/j.biomaterials.2004.11.056

[6] Daculsi G, Laboux O, Malard O, Weiss P. Current state of the art of biphasic calcium phosphate bioceramics. Journal of Materials Science. Materials in Medicine. 2003;**14**(3):195-200. DOI: 10.1023/a:1022842404495

[7] Grgurevic L, Pecina M, Vukicevic S, Marshall R. Urist and the discovery of bone morphogenetic proteins. International Orthopaedics.

2017;**41**(5):1065-1069. DOI: 10.1007/s00264-017-3402-9

[8] Hench LL, Splinter RJ, Allen WC, Greenlee TK. Bonding mechanisms at the interface of ceramic prosthetic materials. Journal of Biomedical Materials Research. 1971;**5**(6):117-141. DOI: 10.1002/jbm.820050611

[9] LeGeros RZ, Silverstone LM, Daculsi G, Kerebel LM. *In vitro* caries-like lesion formation in F⁻ containing tooth enamel. Journal of Dental Research. 1983;**62**(2):138-144. DOI: 10.1177/00220345830620021101

[10] Knowles JC. Phosphate based glasses for biomedical applications. Journal of Materials Chemistry. 2003;**13**(10):2395-2401. DOI: 10.1039/B307119G

[11] Gurusamy R, Sankaralingam P. Inventors; Pandian Bio-Medical Research Centre, assignee. Bioactivity of Fluorophosphate Glasses and Method of Making Thereof. 2015 Jun 18.WO2015087345A1

[12] Kasper FK, Tanahashi K, Fisher JP, Mikos AG. Synthesis of poly (propylene fumarate). Nature Protocols. 2009;**4**(4):518-525. DOI: 10.1038/nprot.2009.24

[13] Siva Kaylasa Sundari S, Shamim Rishwana S, Poornimadevi S, Vijayakumar CT. Synthesis of macromolecular brush and its thermal degradation studies. International Journal of Polymer Analysis and Characterization. 2022;**27**(3):147-157. DOI: 10.1080/1023666X.2022.2029263

[14] Kashif I, Soliman AA, Sakr EM, Ratep A. Effect of different conventional melt quenching technique on purity of

lithium niobate (LiNbO$_3$) nano crystal phase formed in lithium borate glass. Results in Physics. 2012;**2**:207-211. DOI: 10.1016/j.rinp.2012.10.003

[15] Rodrigues N, Benning M, Ferreira AM, Dixon L, Dalgarno K. Manufacture and characterisation of porous PLA scaffolds. Procedia Cirp. 2016;**49**:33-38. DOI: 10.1016/j.procir.2015.07.025

[16] Khang G, Kim MS, Lee HB. A manual for biomaterials/scaffold fabrication technology. World Scientific Publishing Company Singapore; 2007 Jul 3. https://doi.org/10.1142/6408. ISBN: 978-981-3101-60-9

[17] Bejarano J, Detsch R, Boccaccini AR, Palza H. PDLLA scaffolds with Cu-and Zn-doped bioactive glasses having multifunctional properties for bone regeneration. Journal of Biomedical Materials Research Part A. 2017;**105**(3):746-756. DOI: 10.1002/jbm.a.35952

[18] Oh SA, Kim SH, Won JE, Kim JJ, Shin US, Kim HW. Effects on growth and osteogenic differentiation of mesenchymal stem cells by the zinc-added sol-gel bioactive glass granules. Journal of tissue engineering. 2010;**1**(1):475260. DOI: 10.4061/2010/475260

[19] Trivedi S, Srivastava K, Gupta A, Saluja TS, Kumar S, Mehrotra D, et al. A quantitative method to determine osteogenic differentiation aptness of scaffold. Journal of Oral Biology and Craniofacial Research. 2020;**10**(2):158-160. DOI: 10.1016/j.jobcr.2020.04.006

[20] Florencio-Silva R, Sasso GR, Sasso-Cerri E, Simões MJ, Cerri PS. Biology of bone tissue: Structure, function, and factors that influence bone cells. Bio Med Research International 2015;**2015**:17. Article ID: 421746. https://doi.org/10.1155/2015/421746

[21] Zoch ML, Clemens TL, Riddle RC. New insights into the biology of osteocalcin. Bone. 2016;**82**:42-49. DOI: 10.1016/j.bone.2015.05.046

[22] Cecen B, Kozaci D, Yuksel M, Erdemli D, Bagriyanik A, Havitcioglu H. Biocompatibility of MG-63 cells on collagen,poly-L-lacticacid,hydroxyapatite scaffolds with different parameters. Journal of Applied Biomaterials and Functional Materials. 2015;**13**(1):10-16. DOI: 10.5301/jabfm.5000182

[23] Ronca A, Ambrosio L, Grijpma DW. Design of porous three-dimensional PDLLA/nano-hap composite scaffolds using stereolithography. Journal of Applied Biomaterials and Functional Materials. 2012;**10**(3):249-258. DOI: 10.5301/JABFM.2012.10211

[24] Meretoja VV, Tirri T, Malin M, Seppälä JV, Närhi TO. Enhanced osteogenicity of bioactive composites with biomimetic treatment. BioMed Research International. 2014;**2014**:207676. pp. 1-8 DOI: 10.1155/2014/2076762014:207676

[25] Chiu LH, Lai WF, Chang SF, Wong CC, Fan CY, Fang CL, et al. The effect of type II collagen on MSC osteogenic differentiation and bone defect repair. Biomaterials. 2014;**35**(9):2680-2691. DOI: 10.1016/j.biomaterials.2013.12.005

[26] Dong M, Jiao G, Liu H, Wu W, Li S, Wang Q, et al. Biological silicon stimulates collagen type 1 and osteocalcin synthesis in human osteoblast-like cells through the BMP-2/Smad/RUNX2 signaling pathway. Biological Trace Element Research. 2016;**173**(2):306-315. DOI: 10.1007/s12011-016-0686-3

[27] Wibowo H, Widiyanti P, Asmiragani S. The role of chondroitin sulfate to bone healing indicators and compressive strength. Journal

of Basic and Clinical Physiology and Pharmacology. 2021;**32**(4):631-635. DOI: 10.1515/jbcpp-2020-0406

[28] Sankaralingam P, Sakthivel P, Subbiah A, Periyasamy A, Begam J, Thangavel C. Fluorophosphate bio-glass for bone tissue engineering: *in vitro* and *in vivo* study. Bioinspired, Biomimetic and Nanobiomaterials. 2021;**10**(4):123-131. DOI: 10.1680/jbibn.21.00025

[29] Beherei HH, Mohamed KR, El-Bassyouni GT. Fabrication and characterization of bioactive glass (45S5)/titania biocomposites. Ceramics International. 2009;**35**(5):1991-1997

[30] Ren FZ, Leng Y. Carbonated apatite, type-A or type-B?. In: Key Engineering Materials. Switzerland. Trans Tech Publications Ltd. 2012;**493**:293-297

[31] Hanifi A, Fathi MH. Bioresorbability evaluation of hydroxyapatite nanopowders in a stimulated body fluid medium. Iranian Journal of Pharmaceutical Sciences. 2008;**4**(2):141-148

[32] Xu Z, Hodgson MA, Cao P. Effect of immersion in simulated body fluid on the mechanical properties and biocompatibility of sintered Fe–Mn-based alloys. Meta. 2016;**6**(12):309

[33] Ofudje EA, Adeogun AI, Idowu MA, Kareem SO. Synthesis and characterization of Zn-doped hydroxyapatite: Scaffold application, antibacterial and bioactivity studies. Heliyon. 2019;**5**(5):e01716

[34] Palmroth A, Pitkänen S, Hannula M, Paakinaho K, Hyttinen J, Miettinen S, et al. Evaluation of scaffold microstructure and comparison of cell seeding methods using micro-computed tomography-based tools. Journal of the Royal Society, Interface. 2020;**17**(165):102

[35] Ralis ZA, Watkins G. Modified tetrachrome method for osteoid and defectively mineralized bone in paraffin sections. Biotechnic & Histochemistry. 1992;**67**(6):339-345. DOI: 10.3109/10520299209110046

[36] Chen X, Zhao Y, Geng S, Miron RJ, Zhang Q, Wu C, et al. *In vivo* experimental study on bone regeneration in critical bone defects using PIB nanogels/boron-containing mesoporous bioactive glass composite scaffold. International Journal of Nanomedicine. 2015;**10**:839. DOI: 10.2147/IJN.S69001

[37] Rentsch C, Schneiders W, Manthey S, Rentsch B, Rammelt S. Comprehensive histological evaluation of bone implants. Biomatter. 2014;**4**(1):e27993. DOI: 10.4161/biom.27993

[38] Hsieh MK, Wu CJ, Su XC, Chen YC, Tsai TT, Niu CC, et al. Bone regeneration in Ds-red pig calvarial defect using allogenic transplantation of EGFP-pMSCs–A comparison of host cells and seeding cells in the scaffold. Plo S One. 2019;**14**(7):e0215499. DOI:10.1371/journal.pone.0215499

[39] Sankaralingam P. Inventors; BoneSubstitutes, assignee. A synthetic composite as bone graft and the method thereof. 2021 Sep 02. WO/2021/171315